

Transition probabilities in the X(5) candidate ^{122}Ba

P. G. Bizzeti^{1,2}, A. M. Bizzeti-Sona¹, D. Tonev^{3,4}, A. Giannatiempo^{1,2}, C.A. Ur^{5†}, A. Dewald⁶, B. Melon^{1,2}, C. Michelagnoli^{5,9}, P. Petkov⁴, D. Bazzacco⁵, A. Costin¹⁰, G. de Angelis³, F. Della Vedova³, M. Fantuzi^{7,8}, E. Farnea⁵, C. Fransen⁶, A. Gadea^{3,11}, S. Lenzi^{5,9}, S. Lunardi^{5,9}, N. Marginean^{3††}, R. Marginean^{5††}, R. Menegazzo⁵, D. Mengoni^{5,9†††}, O. Möller¹⁰, A. Nannini², D.R. Napoli³, M. Nespolo^{5,9}, P. Pavan^{5,9}, A. Perego^{1,2}, C.M. Petrache^{7,8†††}, N. Pietralla¹⁰, C. Rossi Alvarez⁵, P. Sona^{1,2}

¹Dip. di Fisica e Astronomia, Università di Firenze; ² INFN, Sezione di Firenze; ³INFN, Laboratori Nazionali di Legnaro; ⁴Institute for Nuclear Research and Nuclear Energy, BAS, Sofia; ⁵INFN, Sezione di Padova; ⁶Institut für Kernphysik der Universität zu Köln; ⁷Dip. di Fisica, Università di Camerino; ⁸INFN, Sezione di Perugia; ⁹Dip. di Fisica, Università di Padova; ¹⁰Institut für Kernphysik, TU Darmstadt. ¹¹IFIC, CSIC – University of Valencia, Spain. [†]On leave from IFIN-HH Bucharest. ^{††} Now at IFIN-HH Bucharest. ^{†††} Now at University of the West of Scotland, Paisley, UK. ^{††††} Now at IPN Orsay, IN2P3-CNRS and Université Paris-Sud, France.

To investigate the possible X(5) character of ^{122}Ba , suggested by the ground state band energy pattern, the lifetimes of the lowest yrast states of ^{122}Ba have been measured, *via* the Recoil Distance Doppler-Shift method. The relevant levels have been populated by using the $^{108}\text{Cd}(^{16}\text{O},2n)^{122}\text{Ba}$ and the $^{112}\text{Sn}(^{13}\text{C},3n)^{122}\text{Ba}$ reactions. The $B(E2)$ values deduced in the present work are compared to the predictions of the X(5) model and to calculations performed in the framework of the IBA-1 and IBA-2 models.

PACS numbers: 21.10.Tg (lifetimes), 27.60.+j (specific nuclei $90 < A < 160$)

INTRODUCTION

The X(5) model, introduced by Iachello [1] in 2001, describes nuclei close to the critical point of the phase transition between spherical and axial prolate shape. Many theoretical and experimental efforts have been already dedicated to the study of the X(5) critical point phenomenon [2–15]. Recent experiments provided evidence that, while several nuclei have a level scheme in agreement with the X(5) model, only a few among them have $E2$ transition strengths which also agree with the model predictions (see, *e.g.* [16]).

The light Ba isotopes are known to belong to a transitional region between spherical and axially deformed nuclei, as shown in Fig. 1, where the ratios $E(4_1^+)/E(2_1^+)$ for $N = 62 - 70$ isotones are reported.

Among them, $^{122}\text{Ba}_{66}$ has been proposed by Fransen *et al.* [6] as a rather good X(5) candidate on the basis of the agreement observed between experimental and predicted level energies.

The main purpose of this work is to test the possible X(5) character of this nucleus by measuring the lifetimes in the ground state (g.s.) band in order to deduce the $E2$ strengths of the transitions de-exciting its levels and, possibly, to identify the excited β band (the $s = 2$ band according to X(5) terminology).

Most of the spectroscopic information on ^{122}Ba available in the literature has been obtained from fusion-evaporation reactions. In an old work the ground-state band was observed up to $J = 12$ [17], while in two more recent works [6, 18] the study has been extended to high

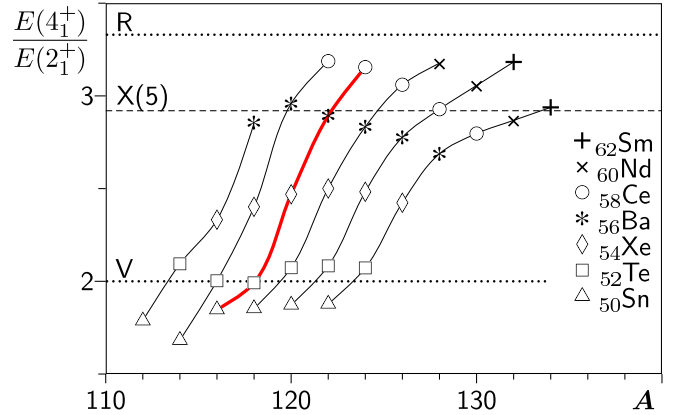


FIG. 1. (Color online) Evolution of the ratio $E(4_1^+)/E(2_1^+)$ as a function of the proton number in the isotope chains with $N = 62, 64, 66, 68, 70, 72$ (from left to right). The data are reported versus $A = N + Z$, to avoid overlapping of the different curves. A thicker line outlines data pertaining to the $N = 66$ isotone chain. Horizontal lines show the theoretical values predicted by harmonic vibrator (V), X(5) model, and rigid rotator (R).

spin states and several bands have been identified.

As to the electromagnetic properties, only the lifetime of the 2_1^+ state has been measured (428 ± 39 ps) from delayed β - γ coincidences in the decay of ^{122}La [19].

To gain additional spectroscopic information on ^{122}Ba three series of measurements have been performed. The

first two experiments have been carried out at the XTU Tandem accelerator of Laboratori Nazionali di Legnaro (LNL) with the GASP array [22], by means of the $^{108}\text{Cd}(^{16}\text{O},2n)^{122}\text{Ba}$ reaction. A thick target was used in the first case, in order to obtain high statistics of double and triple γ coincidences, with the main aim of identifying the 0^+ band head of the $s = 2$ band. In the second one, the lifetimes of the excited levels were measured by the Recoil Distance Doppler-Shift (RDDS) Method, using the Plunger device of the Cologne group. The third measurement, performed at the Tandem accelerator of the Institut für Kernphysik, Cologne, using the $^{112}\text{Sn}(^{13}\text{C},3n)^{122}\text{Ba}$ reaction, was intended to obtain an independent check for the lifetime of the first excited level, which provides the reference value for the normalization of the $B(E2)$ strengths.

Some results of a preliminary evaluation of data have been presented at the Conference CGS13 (Cologne 2008) [21]. Here, we report the final analysis and results, which supersede the previous ones.

EXPERIMENT

Thick-target measurement

The level scheme of ^{122}Ba has been investigated *via* the $^{108}\text{Cd}(^{16}\text{O},2n)^{122}\text{Ba}$ reaction at 62 and 64 MeV beam energy. The target consisted of a 1 mg/cm^2 , 69% enriched ^{108}Cd foil, followed by a 10 mg/cm^2 ^{208}Pb backing. The GASP array was mounted in its Configuration II, *i.e.*, with the Compton suppressed Ge counters at an average distance of 22 cm from the target. Triple and higher-fold coincidence events have been recorded in 55 h of measurement. From the raw data, we have constructed three- and two-dimensional coincidence matrices, containing approximately 1.9×10^7 $E_\gamma - E_\gamma - E_\gamma$ coincidences and 1.5×10^8 $E_\gamma - E_\gamma$ coincidences. These matrices have been used for the search of weak γ transitions in coincidence with known transitions in ^{122}Ba .

Most of the transitions belonging to the bands reported in the previous works [6, 18] have been identified. A revised version of the excitation energy pattern of ^{122}Ba will be presented in a forthcoming paper which will also include the lifetime measurements of the yrast band levels of $J \geq 10$ [20]. Here, we restrict the analysis to the known positive parity bands.

The yrast γ cascade, reported in [18] (see Fig. 2) has been observed at least up to the $20_1^+ \rightarrow 18_1^+$ transition. As to the band based on the 3_1^+ state at 1168 keV, reported by Fransen *et al.* [6], it has been extended by two more transitions. They show the typical angular distribution of stretched E2 transitions and therefore the suggested spin for the corresponding levels are 13 and 15. In addition, a new inter-band transition connecting the 11_1^+ and 10_1^+ states has been found.

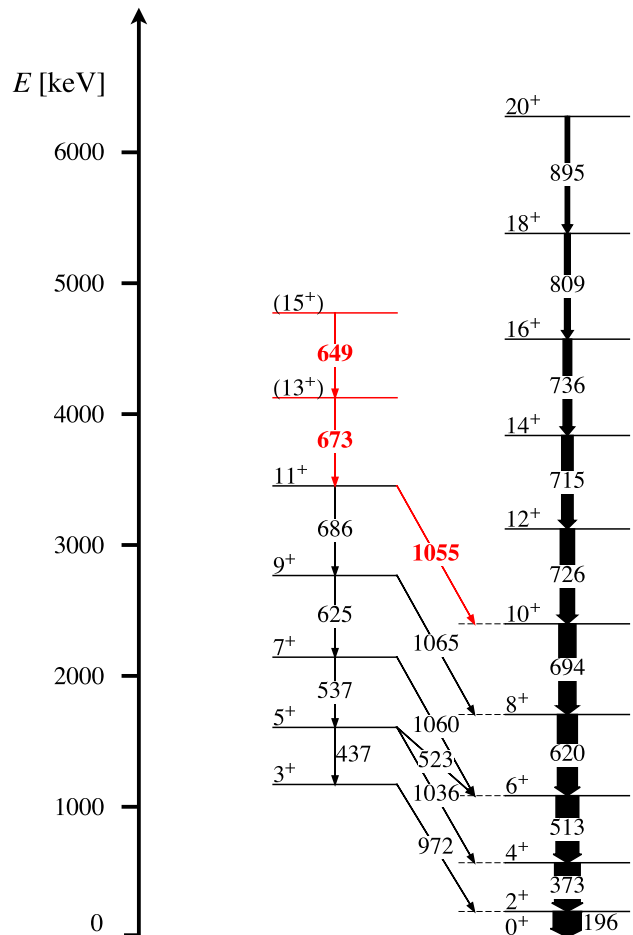


FIG. 2. (color online) Partial level scheme of ^{122}Ba relevant for the present analysis. The two levels on the top of the band based on the 3_1^+ state and the $11_1^+ \rightarrow 10_1^+$ transition have been identified in the present work.

Fransen *et al.* [6] have also observed two γ transitions, of 587 keV and 422 keV, in coincidence with one another and with a 196 keV transition which could originate from the first excited $J = 2^+$ state of ^{122}Ba . In the present measurement, it has been possible to extend the 196, 422, 587 keV cascade to higher lying levels, decaying with γ transitions of 722 keV, 838 keV and 880 keV (in order of decreasing intensity). We have identified the entire cascade as a part of a known band of ^{121}Xe , based on the $7/2^-$ level at 196 keV [23]. Indeed, the ^{121}Xe nucleus is populated in the n2p exit channel of the used reaction.

Moreover, we have observed two transitions, of 199 keV and 514 keV (belonging to the band (4) reported by Petrache *et al.* [18]), which are close in energy to those of the first and third transition of the ground-state band (196 keV and 513 keV, respectively), and are in coincidence with the transitions de-exciting the 8_1^+ and the 6_1^+ levels. In the following, for the sake of simplicity, they will be mentioned as 199 keV-band(4) and 514 keV-band(4) transitions.

In view of the analysis of the data obtained with the RDDS method (described in the following section), for which an overlap of the 514 keV-band(4) and 513 keV transitions could be somewhat problematic, we have determined the relative intensity of the two transitions. They are in coincidence with the $8_1^+ \rightarrow 6_1^+$, 620 keV and the $4_1^+ \rightarrow 2_1^+$, 373 keV transitions. Through an accurate analysis, where a reference transition has been exploited, it has been found that the intensity ratio of the 514 keV-band(4) to the 513 keV line, in coincidence with both the 620 keV and 373 keV transitions, is $(1.6 \pm 0.5) 10^{-2}$, while it is larger $(5.0 \pm 1.4 10^{-2})$ when in coincidence with only the 373 keV transition, due to the fact that several transitions from band (4) of [18] directly feed the 6_1^+ or the 4_1^+ level. Since all the transitions of interest are stretched E2, we expect that their intensity ratio be almost independent of the detector angle.

We have also checked that a weaker $14_2^- \rightarrow 13_2^-$, 371 keV transition in band (3) of [18] has practically no effect on our results.

As to the 0_2^+ state (the band head of the β band), the systematics of heavier barium isotopes (see, *e.g.*, [6, 7]) would suggest an excitation energy of about 1.1 MeV, which is very close to the X(5) prediction. Particular care has been devoted to the search, in the coincidence data, of possible γ rays de-exciting states belonging to the β band. In particular, the energy spectrum gated on the $2_1^+ \rightarrow 0_1^+$ transition has been thoroughly analyzed, but no indication for such γ ray has been found. At the moment, the β band of ^{122}Ba is still to be identified.

Lifetime measurements

In a separate experiment, performed at LNL, the lifetimes of the excited states of the g.s. band in ^{122}Ba have been measured by means of the RDDS method, with the Plunger device of the Cologne group installed in the GASP array (in Configuration 2). Counter rings 1, 2, 6, and 7 (at 34.6° , 59.4° , 120.6° and 145.4° to the beam direction, respectively) provided sufficient separation of the Doppler-shifted part and the unshifted part for most of the γ -ray lines. Excited states in ^{122}Ba were populated *via* the reaction $^{108}\text{Cd}(^{16}\text{O}, 2n)^{122}\text{Ba}$. The target consisted of 0.5 mg/cm^2 ^{108}Cd on a 2.3 mg/cm^2 Ta foil (facing the beam). A 6.4 mg/cm^2 gold foil was used to stop the recoils. The beam energy was 69 MeV and was reduced to about 65 MeV at the entrance in the ^{108}Cd target. Measurements have been performed at 17 target-to-stopper distances, in the range from point of electric contact between target and stopper and $1389 \mu\text{m}$. Since the average velocity of the recoiling nuclei was $v \approx 10^{-2}c$, the corresponding values for the time of flight were in the range $\approx 0.5 \text{ ps} - 463 \text{ ps}$.

Typical examples of the evolution of the line shape with the target-to-stopper distance are shown in Fig. 3.

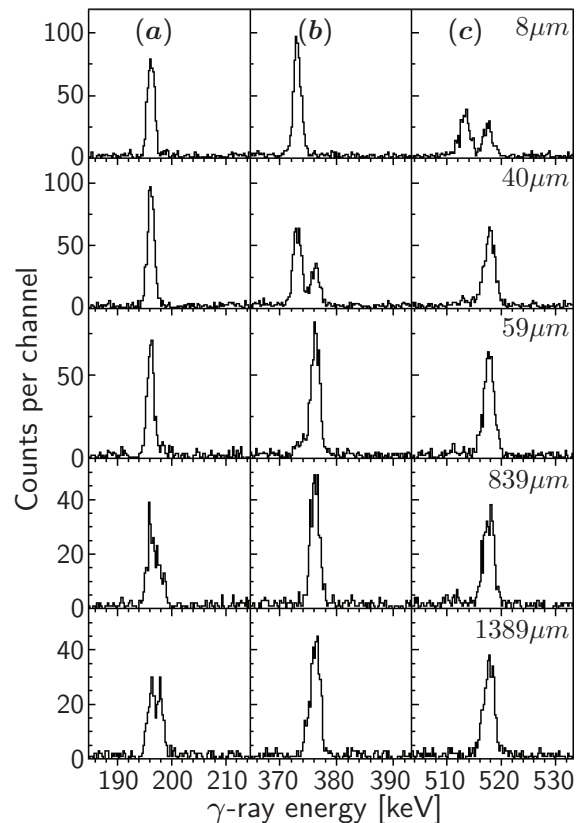


FIG. 3. Evolution of the line shape of the $2_1^+ \rightarrow 0_1^+$ of 196 keV (a), $4_1^+ \rightarrow 2_1^+$ of 373 keV (b), and $6_1^+ \rightarrow 4_1^+$ of 513 keV (c) γ transitions at different target-to-stopper distances, in the experiment performed at LNL. These spectra have been taken at the most forward ring (34.6° with respect to the beam), in coincidence with the Doppler-shifted part of the directly feeding transition. The size of the small 511 keV peak is visible in the lowest part of the right-hand panel.

As to the $2_1^+ \rightarrow 0_1^+$ transition, it is seen that, even at the largest distances, the intensity of the unshifted line is still large and that of the Doppler shifted line is still far from saturation. To extend the data to larger distances, thus improving the reliability of the result, a new measurement has been performed *via* the $^{112}\text{Sn}(^{13}\text{C}, 3n)^{122}\text{Ba}$ reaction, at the Tandem Accelerator of the IKP of the University of Cologne. The target consisted of a 0.3 mg/cm^2 ^{112}Sn layer, evaporated on a 1.7 mg/cm^3 Ta backing (facing the beam). A 4.0 mg/cm^2 gold foil was used to stop the recoiling nuclei. The beam energy was 61 MeV (corresponding to 59 MeV at the entrance in the Sn target). In this case, the average recoil velocity was $v \approx 8 \times 10^{-3}c$. A total of 11 Ge counters were mounted in two rings, 5 at 143 degrees and 6 at 29 degrees, while a further counter was placed at 0 degrees with respect to the beam direction. The average distance of the counters from the target was 11 cm for the backward ring and 20 cm for the forward one. A Plunger device [24], like in the case of the previous mea-

surement, was used. Measurements have been performed at 8 target-to-stopper distances ranging from 10 μm to 3000 μm , so that the significant part of the decay curve of the 2_1^+ state was almost completely included. The quality of the data obtained from this experiment is illustrated in Fig. 4. In spite of the relatively small average recoil velocity the evolution of the unshifted and shifted peaks with increasing target-to-stopper distance is clearly visible.

For the data analysis, the Differential Decay Curve method (DDCM) [25, 26] (described in the next Section) has been used. When necessary, the finite stopping time of the ions in the stopper material (Fig. 5) has been taken into account.

Moreover, a new method, the Integral Decay Curve Method (IDCM) [34] has been exploited in the analysis of the data collected at LNL, concerning the lifetime of the 2_1^+ . Such a method should be particularly advantageous when the most significant points for lifetime evaluation are close to the upper border of the explored range of distances, as in the case considered ¹.

DATA ANALYSIS AND RESULTS

In the RDDS measurements, the lifetime determination is based on the precise knowledge of the areas of the shifted (S) peak, corresponding to the emission of a γ -ray depopulating the investigated level while the recoil nucleus is flying in vacuum or is slowing-down in the target and stopper, and of the unshifted (U) peak, corresponding to an emission when the recoil is at rest in the stopper. In such experiments, the evolution of the intensity splitting between these two components, as a function of the target-to-stopper distance, is sensitive to the lifetime τ of the depopulating level. Such a splitting is shown in Figs. 6-9.

For the lifetime determination, we used the differential decay curve method, proposed in [25, 26]. According to this method, at each target-to-stopper distance x , the lifetime $\tau(x)$ of the level of interest is deduced from quantities obtained directly from the measured data. The method can be applied for data analysis of singles as well as coincidence measurements. A crucial factor for the lifetime determination in RDDS measurements is the precise knowledge of the feeding of the investigated state. In the present analysis lifetimes are always determined using a procedure where a gate is set on the shifted component of a feeding transition. In this way the problem related to an unobserved feeding is completely solved.

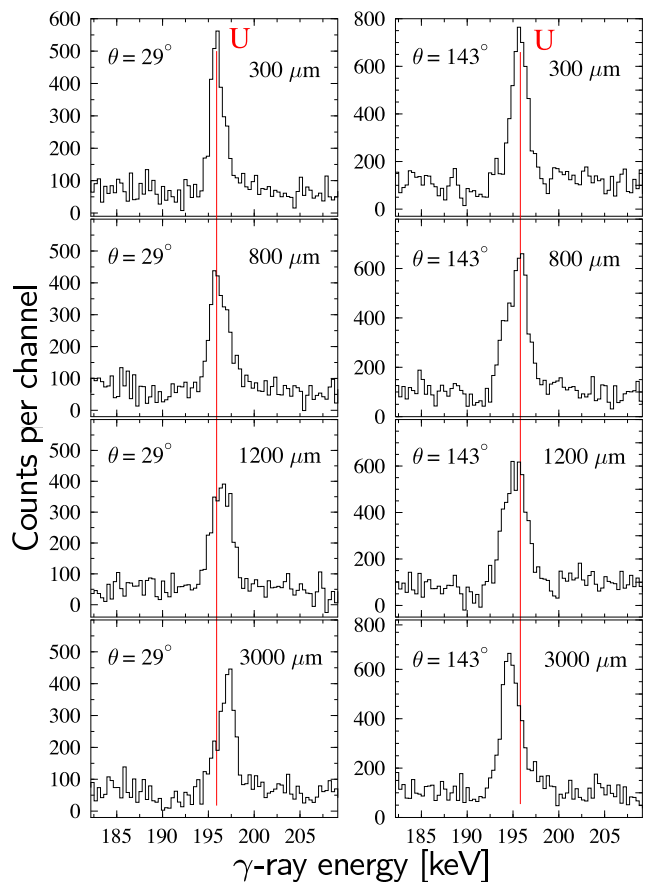


FIG. 4. (Color online) Gated γ -ray spectra of the $2_1^+ \rightarrow 0_1^+$ transition in the experiment performed in Cologne. On the left-hand side, the evolution with the distance of the shifted and unshifted peaks of the $2_1^+ \rightarrow 0_1^+$ transition registered by detectors positioned at an angle of 29° with respect to the beam is shown. On the right-hand side is presented the same evolution registered by detectors positioned at a backward angle of 143° . The position of the unshifted (U) peak is indicated with a vertical line.

Moreover, by gating only on the shifted component of a feeding transition the effect of nuclear de-orientation cancels out completely and does not influence the results of the lifetime analysis [27]. Therefore, special attention has been paid to put a gate only on the shifted component of the feeding transition. When this component was not well separated from the unshifted one, only the part corresponding to the larger values of Doppler shift has been considered. This means to select a fraction of recoil nuclei with an exactly fixed range of the velocities. This fact has been taken into account in the data analysis following the procedure described in [26]. In the choice of the gate, the same range of recoil velocities has been used for the different rings.

In the case of coincidence measurements, as in our experiments, the lifetime can be obtained according to the

¹ This method, in fact, should be free of uncertainties related to the evaluation of derivatives at the border of the region. In addition, it takes automatically into account possible effects due to the angular and velocity spread of the moving nuclei.

equation:

$$\tau(x) = \frac{\{B_s, A_u\}}{\frac{d}{dx}\{B_s, A_s\} <v>} \quad (1)$$

Here, $<v>$ is the mean velocity of the recoils, and the quantities in braces are the numbers of experimental coincident events detected for the shifted (A_s) and unshifted (A_u) part of the transition (A) involved in the analysis, in coincidence with the shifted part of a directly feeding transition (B_s). The derivative in the denominator of Eq. 1 is obtained by fitting a quadratic spline to the intensity of the gated S component.

The precision of the evaluation of the areas of the U- and S-peaks sets limitations on the precision of the investigated lifetimes. The correct determination of these areas, however, depends on several factors, discussed extensively in [28]. Here we only mention the main points which are relevant to the present measurement. In our experiment the beam energy, chosen to ensure a maximal cross-section for the nucleus of interest, leads to recoil velocities v/c around 1%. In such a case the shifted and unshifted peaks for low energy transitions are not well separated and we need to know exactly the lineshapes of the two peaks in order to determine their areas. Whereas the shape of the U-peak is described by the response function of the detector, the shape of the S-peak depends also on all those factors (target thickness, stopping powers, reaction used, beam energy) which determine the velocity distribution of the recoiling nuclei. Also a change in the target-to-stopper distance leads to a modification in the line shape of the shifted peak: the faster recoils reach the stopper earlier and have a higher probability to emit gamma-rays at rest than the slower ones, therefore faster recoils contribute more to the unshifted peak.

For the shorter lifetimes, (*i.e.* < 2 ps) it is important to take into account the finite slowing-down time of the recoils in the stopper. During the slowing-down, the emission of de-exciting γ -rays leads to the appearance of a continuous DSA (Doppler Shift Attenuated) component in the composition of the line-shape which can be described by the procedure published in [28]. As reported in some cases of the $A \approx 130$ mass region [29, 30], taking into account this effect in the analysis has led to a correction of the lifetime values (up to 70 % for very short lifetimes). The importance of the DSA effect in the present measurements is evident in Fig. 9, which shows data concerning the lifetime determination for the 8_1^+ state in ^{122}Ba . For the 8_1^+ (10_1^+) state, the deduced lifetime (limit) turns out to be about 15% longer once the DSA effect has been taken into account.

The precise knowledge of the time evolution of the velocity distribution of the recoils is critical for the description of the line shapes. The best way to obtain this information is by performing a full Monte Carlo (MC) simulation of the creation of the recoils, slowing down in the target, free flight in vacuum, and slowing down

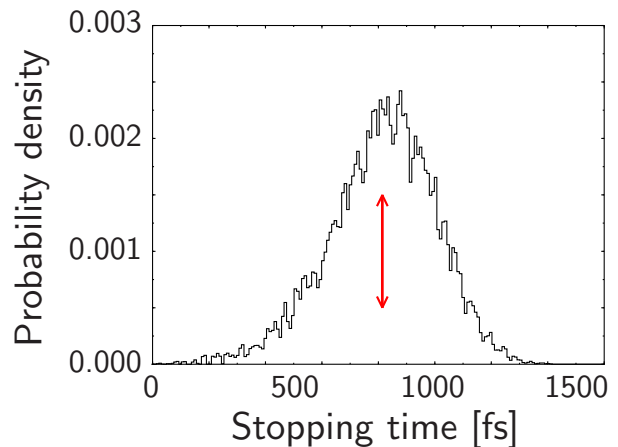


FIG. 5. (color online) Distribution of the stopping time of the ^{122}Ba recoils according to the predictions of the MonteCarlo simulation for 10000 histories. The velocity distribution at the entrance of the gold stopper is calculated for a ^{108}Cd target thickness of 0.5 mg/cm^2 (on a 2.3 mg/cm^2 Ta facing the beam) and a beam energy of 69 MeV at the entrance of the target. The position of the mean value of the stopping time (814 fs) is indicated a vertical arrow.

in the stopper. At a second stage of the MC simulation, the velocity histories are randomized with respect to the two detectors between which the γ - γ coincidences are recorded. Numerical simulations reveal that a summation over 10000 MC-histories is sufficient for a stabilization of the line shapes. We performed a Monte-Carlo simulation of the slowing-down histories of the recoils using a modified [28, 31] version of the program DE-SASTOP [32] which allows for a numerical treatment of the electron stopping powers at ion energies relatively higher than those of the original version. On this basis, a procedure for the analysis of the measured data was developed [28, 31]. In order to fix the stopping power parameters of the target we considered the spectra at large distances, where only shifted peaks are present for shorter lifetimes. Their line-shapes are satisfactorily reproduced by using the simulated velocity distribution. Hence one can conclude that the stopping power of the target material are correctly taken into account. The effect of the momentum carried out by evaporated neutrons from the compound nucleus is also taken into account in the MC procedure. Concerning the slowing-down in the stopper, for the experiment performed at LNL, the mean time interval needed by the recoils to come to rest is predicted to be about 0.8 ps while the whole process is fully completed within about 1.4 ps (see Fig. 5). The time step used for the digitalization of the velocity histories was $\Delta t = 8.87$ fs.

To illustrate the application of the procedure followed in the analysis, we show in Figs. 6-9 examples concerning the lifetime determination for the 196 keV, 373 keV, 513 keV, and 620 keV transitions which depopulate the

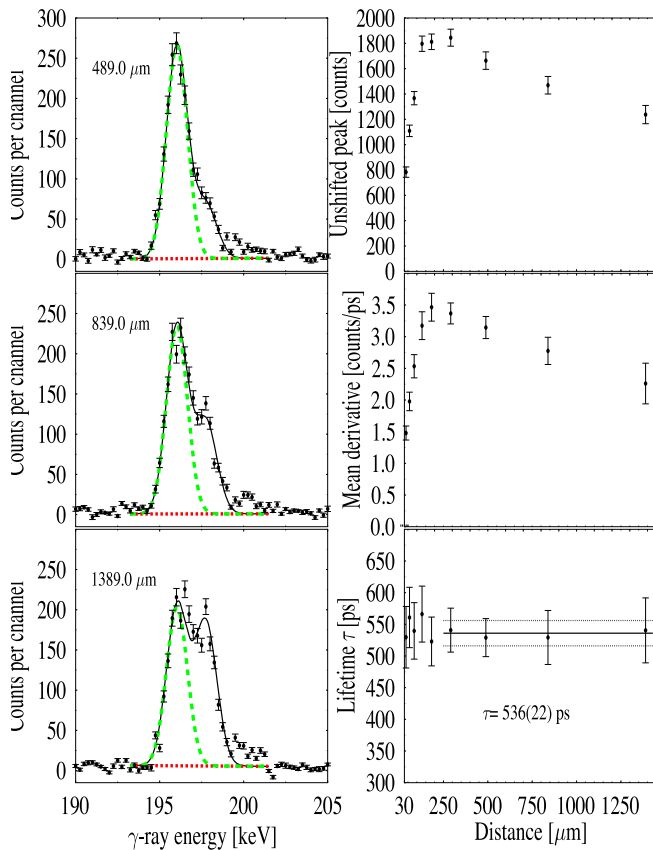


FIG. 6. (Color online) Line-shape analysis of the $2_1^+ \rightarrow 0_1^+$, 196 keV γ -ray transition and determination of the lifetime of the $J^\pi = 2_1^+$ state, according to the procedure presented in [28]. On the left-hand side, spectra measured by the detectors of ring 1 (34.6° with respect to the beam) in coincidence with a part of the shifted component of the $4_1^+ \rightarrow 2_1^+$ transition, also taken on ring 1, and their fit (full line) are shown at three distances. The fits of the unshifted peak and of the background are shown with long-dashed line. The fitted DSA contribution (negligible in this case) is represented with a short-dashed line. The upper panel on the right-hand side (rhs) shows the intensities of the unshifted component of the 196 keV transition, while the curve in the middle panel on the rhs corresponds to the derivative in the denominator of Eq. 1. The points reported in the lower panel correspond to the mean life values deduced at the different distances. The value of τ corresponding to the best fit of results from ring 1 is shown by the central horizontal line and the uncertainty limits are drawn through the sensitivity region.

$J^\pi = 2_1^+, 4_1^+, 6_1^+$, and 8_1^+ levels, respectively. On the left-hand side of the figures, the line shapes, recorded at the indicated distances, are displayed together with the fits. We would like to state that the lifetime value reported in each figure is obtained from the data collected in the ring mentioned in the caption, whereas the corresponding one given in Table I is an average value deduced from the data coming from all the relevant rings.

Possible contaminations of the relevant transitions

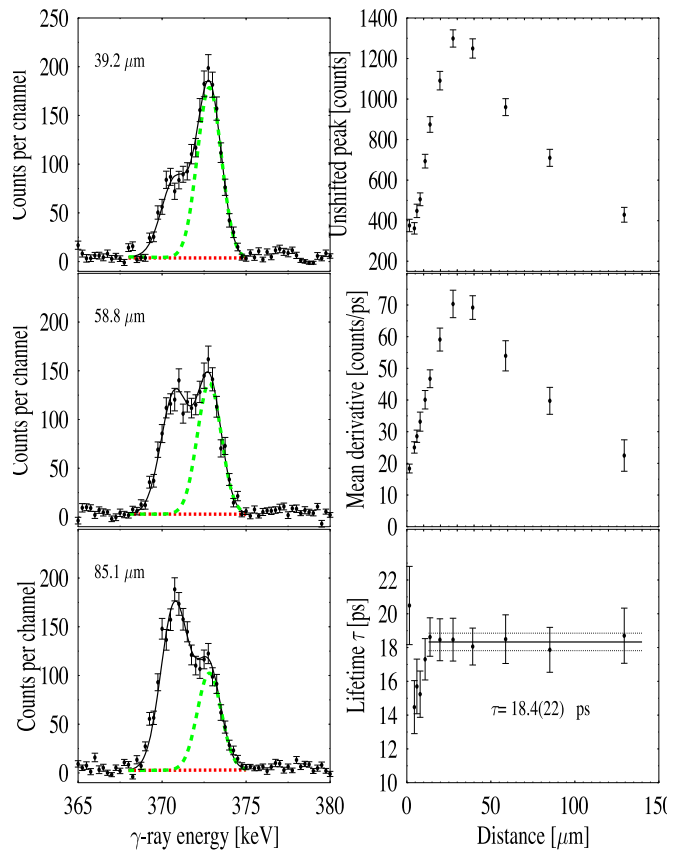


FIG. 7. (Color online) Example of the line-shape analysis of the $4_1^+ \rightarrow 2_1^+$, 373 keV transition and determination of the lifetime of the $J^\pi = 4_1^+$ state. On the left-hand side, spectra in coincidence with a part of the shifted component of the $6_1^+ \rightarrow 4_1^+$ transition, measured by the detectors of ring 7 (145.4° with respect to the beam) and their fit (full line) are shown at three distances. The meaning of the other panels is the same as in Fig. 6.

have been accurately evaluated in the analysis. For the 196 keV, $2_1^+ \rightarrow 0_1^+$ transition they could be due to the 199 keV-band(4) transition or to the known 196 keV transition in ^{121}Xe , populated in the same reaction. To avoid overlapping of the 196 keV line, in coincidence with the shifted part of the 373 keV line, with the 199 keV-band(4) line (which is totally shifted in this case) it has been sufficient to use only the coincidence spectra at the most forward ring. As to the 196 keV transition from ^{121}Xe , we have verified in our triple-coincidence spectra (with double gates on the 196 keV transition and with any one of the transitions of 373 keV, 513 keV and 620 keV) that it is not in coincidence with any transition of energy close to the ones used in our gates for RDDS analysis.

The lifetime of the 2_1^+ level deduced from the measurements performed at LNL is 536 ± 22 ps, where the errors are the statistical ones. With the inclusion of systematic uncertainties we obtain $\tau(2_1^+) = 536 \pm 30$ ps. The value deduced from the Cologne data is fully compatible

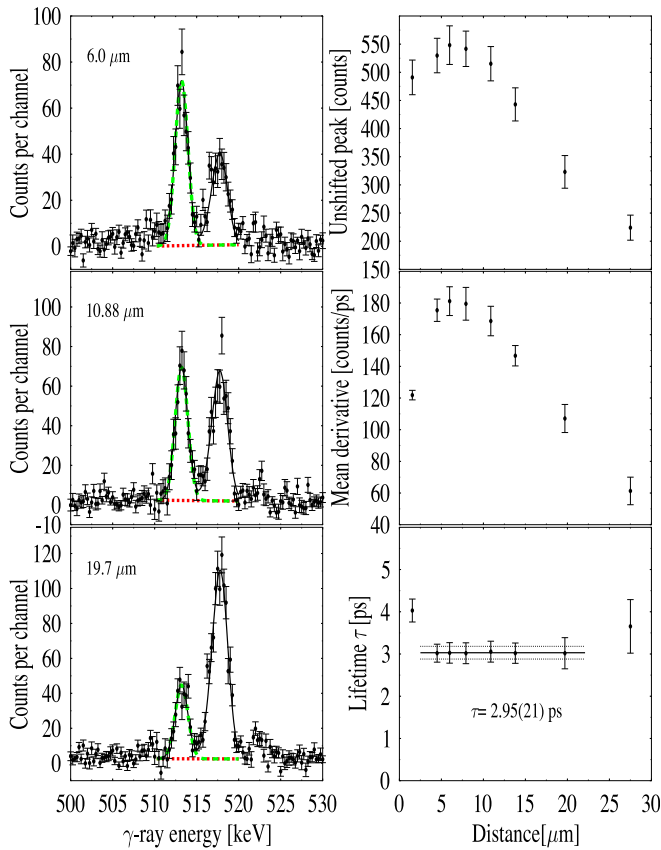


FIG. 8. (Color online) Line-shape analysis of the $6_1^+ \rightarrow 4_1^+$, 513 keV γ -ray transition measured at three different distances and registered by detectors from the forward ring 1 and determination of the lifetime of the $J^\pi = 6_1^+$ state in ^{122}Ba . On the left-hand side the spectra obtained by setting a gate on the shifted component of the 620 keV transition, which feeds directly the level of interest are shown. The meaning of the other panels is the same as in Fig. 6.

with such a result. We observe that the present value is appreciably larger than that ($428 \pm 39\text{ps}$) reported in [19].

An independent evaluation the lifetime of the 2_1^+ state has been performed by exploiting the Integral Decay Curve Method. The data collected at LNL have been analyzed according to the formula [34]

$$\tau = \frac{\int_{x_1}^{x_2} \{B_s, A_u\} dx}{\bar{v}(x_2)\{B_s, A_s\}(x_2) - \bar{v}(x_1)\{B_s, A_s\}(x_1)} \quad (2)$$

extended to the full range of distances. The result (530 ± 30 ps) is in excellent agreement with the one obtained with the DDCM method.

In the analysis concerning the lifetime of the 4_1^+ state we have taken into account the possible bias for the $4_1^+ \rightarrow 2_1^+$ transition, due to the fact that the gate on the shifted part of the 513 keV line includes also the shifted part of the 514 keV-band(4) transition. As only the most shifted part of the 513 keV line has been included in the gate,

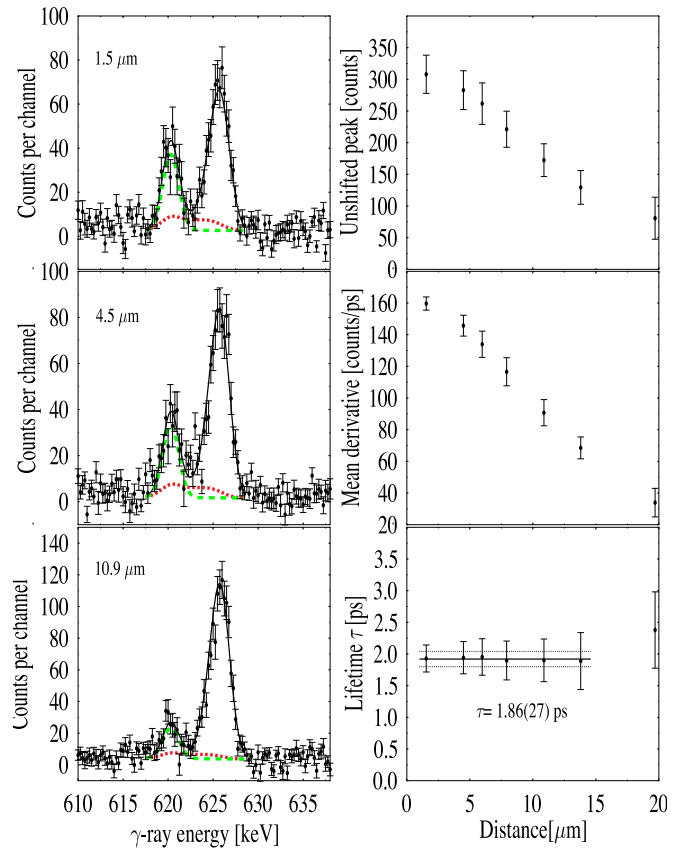


FIG. 9. (Color online) Line-shape analysis of the $8_1^+ \rightarrow 6_1^+$, 620 keV γ -ray transition measured at three different distances and registered by detectors from the forward ring 1 and determination of the lifetime of the $J^\pi = 8_1^+$ state in ^{122}Ba . On the left-hand side the spectra obtained by setting a gate on the shifted component of the 694 keV transition, which feeds directly the level of interest are shown. The importance of the DSA contribution (short-dashed line) is evident. The meaning of the other panels is the same as in Fig. 6.

the fraction of the shifted 514 keV-band(4) line present in this gate can even be somewhat larger than 5%. The largest bias would correspond to a situation in which the 514 keV-band(4) line is fully Doppler shifted while the daughter transitions feeding the 4_1^+ level are completely unshifted. In this extreme situation, the apparent mean life of the 4_1^+ level could be from 10% to 20% longer than the true one, depending on the distance. We therefore evaluated as 20% the error of $\tau(4_1^+)$, on the side of lower values.

Particular attention has been paid to the evaluation of the lifetime of the 6_1^+ state which, as observed in the previous section, can be affected by the presence of the 514 keV-band(4) transition. In coincidence with the *shifted part* of the 620 keV line, only the *shifted part* of the 514 keV-band(4) line is present. It overlaps with the shifted part of the 513 keV line, whose unshifted part remains unaltered. Therefore, the *apparent* time derivative

TABLE I. Values of the lifetimes of excited levels of ^{122}Ba determined in the present work, without (τ_{nc}) and with (τ_{corr}) the correction for the finite slowing-down time of the recoils in the stopper. For the 6_1^+ , the reported value is the average of results obtained from rings 1 and 2; for the 4_1^+ and 8_1^+ states the average is taken over rings 1, 2, 6 and 7. Spin and parity of the relevant states are shown in column 1. Level and transition energies are presented in column 2 and 3, respectively.

State J^π	Energy [keV]	E_γ [keV]	τ_{nc} [ps]	τ_{corr} [ps]
2_1^+	196	196	536 ± 30	536 ± 30
4_1^+	569	373	$18.4^{+2.2}_{-3.7}$	$18.4^{+2.2}_{-3.7}$
6_1^+	1082	513	2.95 ± 0.21	2.95 ± 0.21
8_1^+	1702	620	1.60 ± 0.12	1.86 ± 0.27
10_1^+	2396	694		< 1.62

of the shifted intensity of the 513 keV line will include, in addition, the corresponding derivative of the shifted 514 keV-band(4) line. From the value $1.6 \cdot 10^{-2}$ of the ratio of the 514 keV-band(4) to the 513 keV γ ray, in coincidence with the 620 keV transition, deduced in the previous section, the estimated maximum possible bias on the resulting lifetime turns out to be less than about 2%, much less than the estimated limit of systematic uncertainty. As seen in Fig. 3, there is a small contamination due to the presence of the 511 keV peak. This fact was also the reason for choosing to analyze only the two forward rings, where the shifted peaks are at higher energies.

As to lifetime of the 8_1^+ state, an inspection of Fig. 9 reveals the importance of taking into account the DSA contribution for a precise analysis of the data for short lifetimes.

The attempt to determine the mean life of the 10_1^+ level was based on the analysis of a few results at the shortest distances, which are very sensitive to the evaluation of the background. As a consequence, we can only give an upper limit to the mean life of this level. The results relative to the DSA analysis of the data concerning the 10_1^+ state, which set a lower limit on the lifetime of this level, will be presented in a forthcoming paper[20].

The values of the lifetimes deduced in the present work are shown in Table I together with the upper limit deduced for the 10_1^+ level. Only for the 2_1^+ state a previous value (428 ± 39 ps) was known [19].

The statistical errors on the lifetimes are less than 5% for all the states of interest. The error limits reported in the table include a conservative estimate of the systematic uncertainties, mostly related to the uncertainty in the stopping power. The error limits reported in the tables include an estimate of additional uncertainties related to the background subtraction.

DISCUSSION

At present, one of the most important topics in the study of the nuclear structure concerns the nuclear shape/phase transitions. Its investigation can be performed in the framework of both the collective model [35] and the interacting boson approximation (IBA) model [36]. In the latter case a transition between U(5) and SU(3) symmetries corresponds to a change from a spherical to an axially deformed shape. The evolution of observables in the transitional region exhibits a rather discontinuous behavior and in general its detailed study requires a numerical solution of the Hamiltonian. However, the X(5) model proposed by Iachello [1], based on a simplified Bohr Hamiltonian (in which the β and γ degrees of freedom are decoupled and are associated to a square well potential and a harmonic oscillator potential, respectively) provides an analytic solution which simply describes nuclei near the critical point of the spherical to axially-symmetric rotor transition.

The first identification of nuclei with an X(5) character was that of ^{150}Nd [3] and ^{152}Sm [2], both having $N = 90$. The analysis has been soon after extended to other nuclei around $A \approx 150$ and to other mass regions. It has been found that, in many cases, nuclei having the excitation energies of the g.s. band in good agreement with the predictions of the X(5) model do not have B(E2) values displaying the trend predicted by the model. In particular, in some cases, the B(E2) ratios are close to those of the SU(3) limit (see, e.g. [16, 37–39] and references therein).

A possible identification of ^{122}Ba as a close-to-X(5) nucleus has been proposed by Fransen *et al.* [6]. Indeed, the energy ratio $R_{4/2} = E(4_1^+)/E(2_1^+)$ in the $N = 66$ isotones (see Fig.1) takes in this nucleus the value 2.9 predicted by the model. Moreover, the relative excitation energies of the ground state band as a function of J are in very good agreement with the X(5) predictions. In [6] a tentative identification of the whole $K = 2$ γ -band has been reported and its decay properties have been compared with the predictions of the X(5) model, the O(6) symmetry, and the rotor model. The assignment of the even-J levels of the proposed γ -band to ^{121}Xe , made in the present work, limits the effectiveness of this comparison. Anyway, no definite conclusion about a possible X(5) character of ^{122}Ba was drawn in [6] and the final remark was that this nucleus might have a structure more complicated than expected.

The results obtained in the present work allow to extend the analysis to the electromagnetic transitions probabilities, which provide a very critical and necessary test to establish the structure of a nucleus.

In addition to the X(5) model we have considered the IBA model [36] in both the IBA-1 version, where no distinction is made between proton and neutron bosons, and

the IBA-2 version, where they are considered separately.

To investigate the shape/phase transitions in the framework of the IBA-1 model we used the two-parameter Hamiltonian [40, 41]

$$H = c[(1 - \zeta)(\hat{n}_d) + (\zeta/4N_B)\hat{Q}^{(\chi)} \cdot Q^{(\chi)}] \quad (3)$$

where c is a normalization factor, $\hat{n}_d = d^\dagger \cdot \tilde{d}$, $Q^{(\chi)} = (s^\dagger \tilde{d} + d^\dagger \tilde{s}) + \chi(d^\dagger \tilde{d})$ and N_B is the number of the valence bosons. The same parametrization of the boson quadrupole operator is used in both the Hamiltonian and in the E2 operator (Consistent Q Formalism [42, 43]). The U(5) limit is obtained for $\zeta = 0$ while the SU(3) and O(6) limits are obtained for $\zeta = 1$ and for $\chi = -\sqrt{7}/2$ and 0, respectively.

The calculations have been performed following the same line of [44] and for a boson number $N_B = 11$, corresponding to that of ^{122}Ba , which has 6 protons and 16 neutrons valence nucleons. We first varied ζ from 0 to 1, giving the parameter χ three different values: $-1.32 (= -\sqrt{7}/2)$, -0.75 , and -0.20 . To display the evolution of the nuclear structure for the three cases we report in Fig. 10 the values of $R_{4/2}$ (which is one of the usual benchmarks adopted to characterize the degree of deformation of a nucleus) as a function of ζ . In the figure, the vertical lines mark the values of ζ (0.562, 0.65, and 0.92) where the three curves attain the value predicted by the X(5) model.

By referring to the so-called Casten triangle [45], reported in the inset of Fig. 10, the $\chi = -1.32$ transition is along the U(5) - SU(3) leg. For $\chi = -0.75$, and -0.20 the trajectories are inside the triangle, along lines whose polar coordinates can be deduced from the expressions given in [46], which convert the parameters ζ and χ into the parameters ρ and θ . These polar coordinates allow to span the entire triangle with ρ ranging from 0 [U(5) vertex] to 1 [SU(3) and O(6) vertices] and θ from 0° [SU(3) vertex] to 60° [O(6) vertex]. The values of the parameters ρ and θ , which correspond to the values of χ and ζ ($-1.32, 0.562$), ($-0.75, 0.65$), and ($-0.20, 0.92$) reproducing the X(5) prediction for $R_{4/2}$, are ($0.56, 0^\circ$), ($0.56, 26^\circ$), and ($0.85, 51^\circ$), respectively. The latter case corresponds to a quite γ -soft nucleus.

As a second step, we calculated the values of the energies and $B(E2)$ values of the g.s. band for the three pairs of values of χ and ζ just mentioned. The $E(J)/E(2)$ and $B(E2; J \rightarrow J-2)/B(E2; 2_1^+ \rightarrow 0_1^+)$ ratios are shown, as a function of J , in Fig. 11, together with the predictions of the X(5) model and the U(5) and SU(3) limits. It is seen that the IBA-1 values of $E(J)/E(2)$, which are very close for the three cases considered, are slightly higher than those of the X(5) model and that the normalized $B(E2)$ values slowly decrease from [a] to [c] and approach the values of the SU(3) limit.

As to the analysis in the framework of the IBA-2 model, we kept the Hamiltonian parameters fixed to

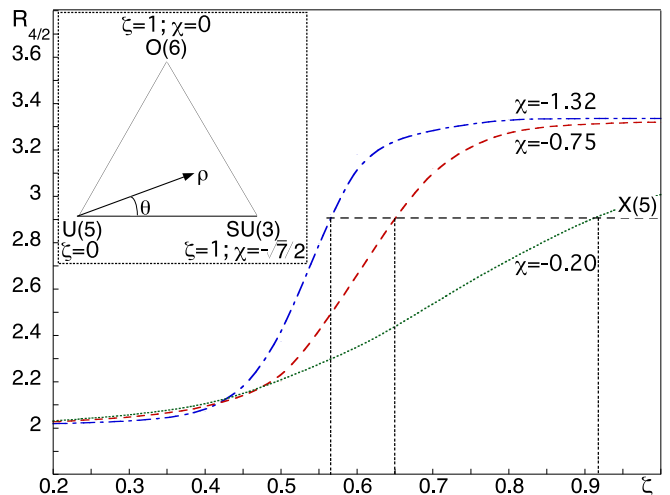


FIG. 10. (Color online) The ratio $R_{4/2}$ is shown as a function of ζ for the three indicated values of χ and $N_B = 11$. The horizontal line shows the value predicted by the X(5) model, the vertical lines mark the values of ζ for which $R_{4/2}$ takes the value predicted by the X(5) model. In the inset the Casten triangle is displayed.

those found in the studies of the whole Te, Xe, Ba isotopic chains [47, 48]. In this way a possible agreement due to a fine tuning of the model parameters to the experimental data can be excluded. We used the same Hamiltonian as in [47] with the addition of the Majorana term $\hat{M}_{\pi\nu}$

$$H = \varepsilon(\hat{n}_{d_\pi} + \hat{n}_{d_\nu}) + \kappa \hat{Q}_\pi^{(\chi_\pi)} \cdot \hat{Q}_\nu^{(\chi_\nu)} + \hat{M}_{\pi\nu}(\xi_1, \xi_2, \xi_3) \quad (4)$$

The Majorana parameters ξ_i have been kept at 1 MeV so as to push at high energies states non symmetric in the proton-neutron degrees of freedom. The values adopted for the parameters ε (0.5 MeV), κ (-0.21 MeV), χ_ν (0.1), χ_π (-0.5) are those deduced in [47] for ^{122}Ba . The values of χ_ν and χ_π in the E2 transition operator

$$\hat{T}(E2) = e_\nu \hat{Q}_\nu^{(\chi_\nu)} + e_\pi \hat{Q}_\pi^{(\chi_\pi)} \quad (5)$$

are the same as in the Hamiltonian (CQF [42, 43]). The proton- and neutron-boson effective charges, for which no value is reported in [47, 48] for ^{122}Ba , have been kept at the values $e_\pi = 0.18$ eb and $e_\nu = 0.095$ eb, respectively. They are slightly higher than those evaluated microscopically in [48] for the isotone ^{120}Xe . It is important to notice that a 50% variation of the parameters e_π and/or e_ν changes by less than $\sim 1\%$ the relevant $B(E2)$ ratios so that, in this comparison, basically no free parameters were used.

The $B(E2)$ values calculated in the framework of the IBA-2 model and those predicted by the X(5) model are compared to the experimental ones in Table II.

The energies ratios and the $B(E2)$ ratios are shown in Fig. 11 as a function of J . It is seen that the agreement between experimental and calculated energy ratios is comparable to that obtained by the X(5) model. The

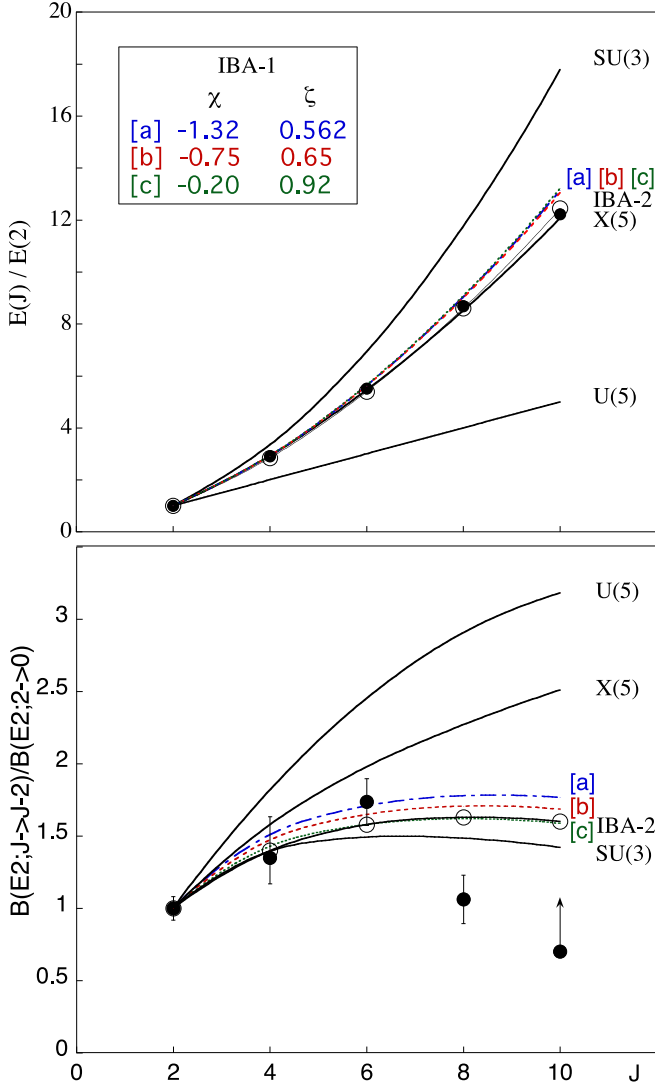


FIG. 11. (Color online) The experimental values (black full circles) of the energy ratios (upper part) and $B(E2)$ ratios (lower part) of the g.s. band of ^{122}Ba are compared with the X(5), U(5) and SU(3) predictions (full lines), with the IBA-1 calculations (dashed lines [a], [b] and [c]) and with the IBA-2 calculations (open circles). The values of the parameters χ and ζ used in the IBA-1 calculations are given in the inset.

trend of the calculated $B(E2)$ ratios is similar to that obtained in the IBA-1 calculations (with values very close to those corresponding to parameters [c] in IBA-1) and that of both IBA predictions is close to that of the SU(3) model. The IBA calculations are thus able to describe the energy ratios at a level close to that of the X(5) model and the $B(E2)$ ratios at a level not too far from that of the SU(3) symmetry, which, however, overestimates the $B(E2)$ ratio of the 8_1^+ state. On the other hand, the predictions of the X(5) model, which are compatible with the experimental $B(E2)$ ratios up to $J = 6$, are hardly compatible with the experimental value for $J = 8$.

A precise value of the lifetime of the 10_1^+ state would be

TABLE II. Values of the reduced transition strengths $B(E2)$ in the g.s. band of ^{122}Ba , compared with the results of the IBA-2 calculation described in the text, and with the predictions of the X(5) model (which has been normalized to the experimental value for the $2_1^+ \rightarrow 0_1^+$ transition).

Transition	E_γ [keV]	$B(E2)_{exp}$ [e^2b^2]	$B(E2)_{IBA-2}$ [e^2b^2]	$B(E2)_{X(5)}$ [e^2b^2]
$2_1^+ \rightarrow 0_1^+$	196	0.45 ± 0.03	0.43	0.45
$4_1^+ \rightarrow 2_1^+$	373	$0.60^{+0.12}_{-0.07}$	0.62	0.72
$6_1^+ \rightarrow 4_1^+$	513	0.77 ± 0.06	0.69	0.89
$8_1^+ \rightarrow 6_1^+$	620	0.47 ± 0.07	0.71	1.03
$10_1^+ \rightarrow 8_1^+$	694	≥ 0.46	0.70	1.13

necessary to clarify whether (and how much) the trend of $B(E2)$ ratios keep decreasing at higher spin values. This, indeed, would allow to perform a more stringent comparison of experimental and theoretical data.

CONCLUSIONS

The lifetimes of the 4_1^+ , 6_1^+ , 8_1^+ levels and an upper limit for the lifetime of the 10_1^+ level of ^{122}Ba have been determined for the first time in the present work. As to the 2_1^+ state, the present mean life $\tau_m = 536 \pm 30$ ps is appreciably longer than that ($\tau_m = 428 \pm 39$ ps) obtained by Morikawa *et al.* [19] by electronic timing.

It has been found that the 587-422-196 keV cascade, tentatively interpreted in [6] as the $4_2^+ \rightarrow 2_2^+ \rightarrow 2_1^+$ cascade in ^{122}Ba , belongs to the ^{121}Xe nucleus. As to the ^{122}Ba , two more levels have been added on top of the band based on the 3_1^+ state.

A description of ^{122}Ba as an X(5)-like nucleus matches very well the behavior of the experimental energies, whereas the data on the $B(E2)$ ratios of the g.s. band obtained in the present work suggest a picture closer to the SU(3) description (which in turn is not compatible with the data on the energies). Both IBA-1 and IBA-2 calculations predict values comparable to those of X(5) for the energies ratios and close to the SU(3) for the $B(E2)$ ratios. To test to what extent a description of the ^{122}Ba nucleus in the framework of the IBA model is close to the experimental data a precise experimental value of the lifetime of the 10_1^+ state would be very valuable.

ACKNOWLEDGMENTS

This research has been supported within the ‘‘Research Infrastructure Action under FP6 - Structuring the European Research Area - Programme, Contract n. 506065 EURONS - EUROpean Nuclear Structure research’’. D.T. and P.P. are indebted to the National Science Fund at the Bulgarian Ministry of Education and

Science under contract number RIC-02/2007 for a financial support.

-
- [1] F. Iachello, Phys. Rev. Lett. **87**, 052502 (2001).
 [2] R.F. Casten and N.V. Zamfir, Phys. Rev. Lett. **87**, 052503 (2001).
 [3] R. Krücken *et al.*, Phys. Rev. Lett. **88**, 232501 (2002).
 [4] P.G. Bizzeti and A. M. Bizzeti-Sona, Phys. Rev. C **66**, 031301(R) (2002).
 [5] C. Hutter *et al.*, Phys. Rev. C **67**, 054315 (2003).
 [6] C. Fransen *et al.*, Phys. Rev. C **69**, 014313 (2004).
 [7] C. Michelagnoli, Thesis (University of Florence, April 2009).
 [8] D. Tonev *et al.*, Phys. Rev. C **69**, 034334 (2004).
 [9] M.A. Caprio, Phys. Rev. C **69**, 044307 (2004).
 [10] E.A. McCutchan *et al.*, Phys. Rev. C **69**, 024308 (2004).
 [11] N. Pietralla and O.M. Gorbachenko, Phys. Rev. C **70**, 011304 (2004).
 [12] A. Dewald *et al.*, J. Phys. G **31**, S1427 (2005).
 [13] D.L. Balabanski *et al.*, Int. J. of Mod. Phys. E **15**, 1735 (2006).
 [14] D. Bonatsos *et al.*, Phys. Lett. B **649**, 394 (2007).
 [15] A.F. Mertz *et al.*, Phys. Rev. C **77**, 014307 (2008).
 [16] R.M. Clark *et al.*, Phys. Rev. C **68**, 037301 (2003).
 [17] J. Conrad *et al.* Nucl. Phys. **A234**, 157 (1974).
 [18] C.M. Petrache *et al.* Eur. Phys. J. **A12**, 135 (2001).
 [19] T. Morikawa *et al.*, Phys. Rev. C **46**, R 6 (1992).
 [20] C. Michelagnoli *et al.* to be published.
 [21] P.G. Bizzeti *et al.*, Proc. of the 13th International Symposium on capture gamma-rays and related topics (Cologne 2008, Eds. A.Blazhev, J. Jolie, N.Warr and A.Zilges, AIP Conf. Proc. 1090) p.352.
 [22] C. Rossi Alvarez, Nuclear Physics News **3**, n.3 (1993).
 [23] NNDC data base, <http://nndc.bnl.gov>.
 [24] A. Dewald *et al.*, Nucl. Phys. A **545**, 822 (1992).
 [25] A. Dewald *et al.*, Z. Phys. A **334**, 163 (1989).
 [26] G. Böhm, A. Dewald, P. Petkov and P. von Brentano, Nucl. Instrum. Methods Phys. Res. A **329**, 248 (1993).
 [27] P. Petkov, Nucl. Instrum. Methods Phys. Res. A **349**, 289 (1994).
 [28] P. Petkov *et al.*, Nucl. Instrum. Methods Phys. Res. A **431**, 208 (1999).
 [29] T. Klemme *et al.*, Phys. Rev. C **60**, 034301 (1999).
 [30] P. Petkov *et al.*, Phys. Rev. C **62**, 014314 (2000).
 [31] P. Petkov *et al.*, Nucl. Phys. **640**, 293 (1998).
 [32] G. Winter, Nucl. Instrum. Methods **214**, 537 (1983).
 [33] W.M. Currie, Nucl. Instrum. Methods **73**, 173 (1969).
 [34] P.G. Bizzeti, Improved method of analysis of Recoil Distance measurements of nuclear lifetimes, Annual Report 2008 of LNL; and to be published.
 [35] A. Bohr and B. Mottelson, *Nuclear Structure* (Benjamin, Reading, MA, 1975), Vol. II, p.1.
 [36] F. Iachello and A. Arima, *The Interacting Boson Model* (Cambridge University Press, Cambridge, England 1987) and references therein.
 [37] A. Dewald *et al.*, Eur. Phys. J. A **20**, 173 (2004).
 [38] E.A. McCutchan, N.V. Zamfir, R.F. Casten, M.A. Caprio, H. Ai, H. Amro, C. W.Beausang, A.A. Hecht, D.A. Meyer, J.J. Ressler, Phys.Rev. C **71**, 024309 (2005).
 [39] E. A. McCutchan *et al.*, Phys. Rev. C **73**, 034303 (2006).
 [40] N. V. Zamfir, P. von Brentano, R.F. Casten, and J. Jolie, Phys. Rev. C **66**, 021304 (2002).
 [41] V. Werner, P. von Brentano, R.F. Casten, and J. Jolie, Phys. Lett. **B527**, 55 (2002).
 [42] D.D. Warner and R.F. Casten, Phys. Rev. C **28**, 1798 (1983).
 [43] P. O Lipas, P. Toivonen, and D. D. Warner, Phys. Lett. **155B**, 295 (1985).
 [44] E. A. McCutchan, N. V. Zamfir, and R. F. Casten, Phys. Rev. C **71**, 034309 (2005).
 [45] R.F. Casten, in *Interacting Bose-Fermi Systems in Nuclei*, edited by F. Iachello (plenum, New York, 1981), p.3. (1983). **155B**, 295 (1985).
 [46] E. A. McCutchan, N. V. Zamfir, and R. F. Casten, Phys. Rev. C **69**, 064306 (2004).
 [47] T. Otsuka, *Algebraic Approaches to Nuclear Structure* (Ed. R.F. Casten, Brookhaven National Laboratory Upton, New York, USA 1993) and T. Otsuka, Nucl. Phys. A **557**, 531 (1993).
 [48] T. Mizusaki and T. Otsuka, Prog. Theor. Phys. Suppl. **125**, 97 (1996).